Preprints of the 21st IFAC World Congress (Virtual)
Berlin, Germany, July 12-17, 2020

Fully Robust Sensorless Control of Direct-Drive PMSG Wind Turbine Feeding a Water Pumping System

Benzaouia Soufyane* **. Rabhi Abdelhamid. Zouggar Smail*. M. L. Elhafyani*. Ahmed El Hajjaji****
** Laboratory of Electrical Engineering and Maintenance – LEEM, University Mohammed 1st, High School of Technology Oujda, Morocco (e-mail: soufyane.benzaouia@gmail.com)*
*** Laboratory of Modelisation, Information and Systems – MIS, University of Picardie Jules Verne, 33 rue Saint Leu, 80039 Amiens Cedex, France*

Abstract: In this paper, we propose a fully sensorless control strategy that guarantees robustness and stability properties. The aim is to maximize the extracted power and to ensure an optimum control without mechanical sensors to reduce the cost. Firstly, a fuzzy logic technique has been used to estimate the wind speed information. Then an improved model reference based on adaptive sliding mode controller has been developed to estimate the permanent-magnet synchronous generator speed. The proposed control strategy includes two control loops, an outer control loop based on fuzzy super twisting algorithm to regulate the generator speed to its optimal value and to provide the optimum *DC* side current, and an internal control loop based on sliding mode controller to regulate the *DC* side current to its optimal value and provides the appropriate signal for the *DC-DC* boost converter. The considered system in this work is supposed supplying a water pumping system for a use in isolated areas. The proposed control strategy has been compared to the conventional *MPPT* control method based on the concept of perturbation and observation. The obtained results show, a good estimation performance for the wind speed estimator and the improved *MRAS* speed observer, a good tracking performance and a good stability around the maximum power point. Comparing to the classical *MPPT* strategy, the current technique can greatly reduce the ripples that can generate vibrations and significant noise on the generator and the motor-pump group.

Keywords: *PMSG*, *PMDC*, Centrifugal pump, Water pumping, Wind energy, *P&O*, *MRAS* observer, Fuzzy logic controller (*FLC*) , Sliding mode controller (*SMC*), Variable gain super twisting algorithm (*VGSTA*).

1. INTRODUCTION

Wind energy has received a great deal of attention as an ideal alternative to conventional energy sources. Pumping water is one of the most promising application for wind energy conversion systems. Permanent magnet synchronous generator (*PMSG*) based wind turbines are the most preferred for standalone applications due to their high reliability and efficiency. Small commercial *PMSG* wind turbines already contain an internal rectifier. The accessible output provides a *DC* voltage. The connection of a *DC* motor driving a centrifugal pump is the most low cost solution, avoiding by that the need of an inverter in the case of using an *AC* motors (Fernandez et al. 2003). The final wind electric water pumping system configuration is illustrated in Figure (1). Its consists of permanent-magnet synchronous generator, an *AC/DC* converter, a *DC-DC* boost converter and a centrifugal pump driven by a permanent-magnet *DC* (*PMDC*) motor .This pumping system can operate autonomously; no additional power source is needed for the excitation circuit of the two machines.

The major drawback of wind turbine systems is the highly nonlinear behavior (Figure (2)). The main objective is to maximize the energy capture at every wind speed. Conventional *MPPT* control strategies have shown a poor performance and a low efficiency under random wind speed profile and external disturbances. In literature, several *MPPT* control strategies were developed and proposed in order to extract the maximum available power from the wind. The main problem is the use of mechanical sensors. According to (Qiao et al.,2011), the use of such sensors increases the overall cost of the wind system and the failure rate. The best alternative is to use an observer or an estimator. In (Sitharthan et al.,2019) an adaptive hybrid intelligent *MPPT* controller is proposed, the developed strategy allows to estimate the effective wind speed and the optimal rotor speed of the wind power generation system by the *RBFNN* technique. In (Belmokhtar et al.,2014), a novel *FLC MPPT* method has been proposed, an *MRAS* observer based on fuzzy logic technique has been used to estimate the *DFIG* rotor's speed, and then the wind speed has been estimated from the mechanical power using the fuzzy logic technique. In (Qiao et al.,2011) a sensorless control strategy is proposed for a directly driving permanent magnetic generator, a sliding-mode observer is designed to estimate the generator rotor position and a back-propagation artificial neural network (*BPANN*) is designed to estimate the wind speed. In (Mohamed, Mansouri, et al.,2019), a new hybrid sensorlees speed control is proposed for a non-salient pole *PMSG* wind turbine, the generator speed is estimated by a hybrid structure that combines two observers and a switching algorithm.

In this paper, the rotational generator speed is estimated through an improved *MRAS* observer based on a sliding mode controller adaptation mechanism and a fuzzy estimator is used to estimate the effective wind speed. The proposed control strategy includes two control loops, a speed controller to regulate the rotational speed to its optimal value and to provide the optimum (reference) *DC* side current as output and a

current controller used to regulate the *DC* side current to its optimal value and to provide the appropriate duty cycle to the *DC-DC* boost converter. Unlike the considered conventional constant gain proportional integral (*PI*) controllers in (Kot et al., 2013), this work proposes a robust variable gain super twisting algorithm assisted with a fuzzy logic controller and a sliding mode controller in order to improve the system stability and to reduce the convergence time. The effectiveness of the proposed control strategy is checked by several computer simulation tests using *Matlab/Simulink* software and compared to the conventional *MPPT* strategy.

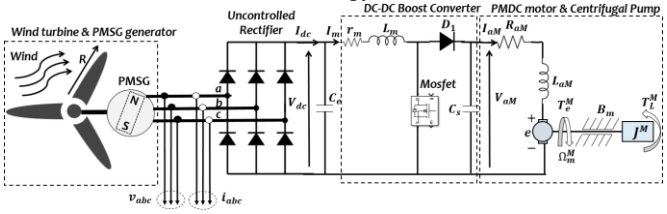

Figure 1. Studied wind electric water pumping system

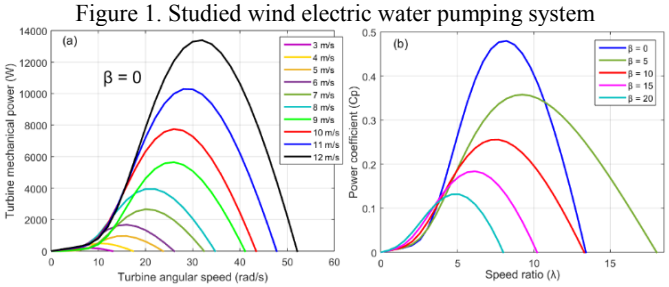

Figure 2. a. Wind generator power curves at various wind speed, b. Characteristics C_p vs λ for different values of the pitch angle β.

2. MODELING OF WIND ELECTRIC WATER PUMPING SYSTEM

2.1 Modeling of the Wind Turbine

The model of the turbine is given by following equations:

$$p_v = \frac{(\rho . A . {v_w}^3)}{2} \tag{1}$$

$$p_m = \frac{1}{2} C_p(\lambda, \beta) . \rho . A . {v_w}^3 \tag{2}$$

$$\lambda = \frac{\Omega_m^G R}{v_w} \tag{3}$$

$$\begin{cases} C_p(\lambda, \beta) = C_1 \left(\frac{C_2}{\gamma} - C_3 . \beta - C_4 \right) e^{\frac{-C_5}{\gamma}} + C_6 . \lambda \\ \frac{1}{\gamma} = \frac{1}{\lambda + 0.08\beta} - \frac{0.035}{\beta^3 + 1} \end{cases} \tag{4}$$

$$T_m^G = \frac{p_m}{\Omega_m^G} = \frac{1}{2 . \Omega_m^G} C_p(\lambda, \beta) . \rho . A . {v_w}^3 \tag{5}$$

$$\begin{cases} T_m^G = J^G \dot{\Omega}_m^G + f . \Omega_m^G + T_{em}^G \\ J^G = J_{turbine}^G + J_g^G \end{cases} \tag{6}$$

Where p_v is the wind power, ρ is the air density, A is the circular area, v_w is the wind speed, p_m is the mechanical power, C_p is the power coefficient, β is the pitch angle, λ is the tip speed ratio, Ω_m^G is the turbine rotor speed, R is the turbine radius, T_m^G is the mechanical torque, T_{em}^G is the electromagnetic torque produced by the generator, f is the friction coefficient and J^G is the total moment of inertia of the rotating parts.

2.2 Permanent Magnet Synchronous Generator (PMSG) model

d-q stator voltage equations of this generator are given by the following expressions:

$$\begin{cases} V_{ds} = R_s I_{ds} + L_d \dot{I}_{ds} - \omega_r \psi_{qs} \\ V_{qs} = R_s I_{qs} + L_q \dot{I}_{qs} + \omega_r \psi_{ds} \\ \psi_{ds} = L_d I_{ds} + \psi_0 \\ \psi_{qs} = L_q I_{qs} \end{cases} \tag{7}$$

Differential equations of the *PMSG* can be obtained as follows:

$$\begin{cases} L_d \dot{I}_{ds} = V_{ds} - R_s I_{ds} + \omega_r L_q I_{qs} \\ L_q \dot{I}_{qs} = V_{qs} - R_s I_{qs} - \omega_r L_d I_{ds} - \psi_0 \omega_r \end{cases} \tag{8}$$

The electromagnetic torque is represented by:

$$T_{em}^G = \frac{3}{2} p \left[(L_d - L_q) I_{ds} I_{qs} + \psi_0 I_{qs} \right] \tag{9}$$

$$T_{em}^G = \frac{3}{2} p \psi_0 I_{qs} \ , \ (L_d = L_q) \tag{10}$$

Where L_d, L_q are the inductances of the generator on the q and d axis, R_s is the stator resistance, ψ_0 is the permanent magnetic flux, ω_r is the the electrical rotating speed of the *PMSG* which is given by $\omega_r = p . \Omega_m^G$ and p is the number of pole pairs.

2.3 Permanent-Magnet DC Motor (PMDC) and Centrifugal pump model

The model of the *PMDC* motor is represented by the following equations:

$$\begin{cases} V_{aM} = R_{aM} I_{aM} + L_{aM} \dot{I}_{aM} + e \\ T_e^M = K_t I_{aM} \\ e = K_e \Omega_m^M \\ T_e^M - T_L^M = J^M \dot{\Omega}_m^M + B_m . \Omega_m^M + T_f^M \end{cases} \tag{11}$$

The load torque of the centrifugal pump is given by the following expression:

$$T_L^M = a . {\Omega_m^M}^n + b \tag{12}$$

Where R_{aM} is the armature winding resistance, L_{aM} is the armature self-inductance, I_{aM} is the motor armature current, V_{aM} is the applied voltage, e is the back *e.m.f* of the *PMDC* motor, K_e is the voltage constant, Ω_m^M is the angular speed, K_t is the torque constant, J^M is the moment of inertia, B_m is the viscous torque constant, T_f^M is the torque constant for rotational losses, T_e^M, T_L^M are the electromagnetic torque and load torque respectively, and a, b are the constants of the pump.

3. FUZZY WIND SPEED ESTIMATOR

The fuzzy inference system of the wind speed estimator receives the error between the estimated mechanical power $\hat{P}_{m_{opt}}$ and the calculated one $P_{m_{opt}}^c$ using the generated estimated wind speed $\hat{v}_w$ provided by the *FLC* as a feedback. The error between the estimated mechanical power and the calculated one is multiplied to a scaling factor μ and then considered as input to the *FIS*, this error is calculated as follows:

$$\mu . x_{p_m} = \mu . (\hat{P}_{m_{opt}} - P_{m_{opt}}^c) \tag{13}$$

$$Where: P_{m_{opt}}^c = \frac{1}{2} C_{p_{max}}(\lambda_{opt}) . \rho . A . {\hat{v}_w}^3 \tag{14}$$

The estimation process of the wind speed requires the turbine mechanical power information. This information can be estimated here using two ways. The first method by using equation (15), this technique is no longer recommendable because its requires the torque information, and it will causes an additional cost for installing a torque sensor, and the second method uses equations (16), which represents the conversion of the turbine mechanical power in the generator electrical power and consider power losses p_{loss} in the model of the generator (Qiao et al.,2011). Power losses p_{loss} can be divided

into four parts, copper loss p_{copper} in the stator windings, which can be calculated using equation (18), the mechanical loss, which is assumed to be 1.0% of electrical power p_e, the core loss that depends on the flux linkage and the rotor speed, and the stray load loss that is also assumed to be 1.0% of electrical power p_e (Qiao et al.,2011).

$$\hat{P}_{m_{opt}} = T^G_{m_{ref}} \hat{\Omega}^G_m \quad (15)$$

$$\hat{P}_{m_{opt}} = J^G \hat{\Omega}^G_m . \dot{\hat{\Omega}}^G_m + p_{e_{opt}} + p_{loss} + f \hat{\Omega}^{G\,2}_m \quad (16)$$

$$p_e = \frac{3}{2}\left(V_{ds} I_{ds} + V_{qs} I_{qs}\right) \quad (17)$$

$$p_{copper} = \frac{3}{2}\left(I^2_{qs} R_s + I^2_{ds} R_s\right) \quad (18)$$

$\hat{\Omega}^G_m$ represents the estimated generator rotational speed provided by the improved *MRAS* observer. Details about this observer will be discussed in the next section.

The basic structure of the *FLC* controller consists of *Fuzzification* process, an Inference engine, a knowledge base and a *Defuzzification* process. The used *FLC* here is composed of one input and one output variable. The *FLC* input receive error $(\mu.x_{p_m})$ between $\hat{P}_{m_{opt}}$ and $P^c_{m_{opt}}$, and the output of the *FLC* provides the change of the estimated wind speed $(\Delta\hat{v}_w(k))$, and the estimated wind speed is obtained using the following equation:

$$\hat{v}_w(k) = \hat{v}_w(k-1) + \Delta\hat{v}_w(k) \quad (19)$$

Input error variable $(\mu.x_{p_m})$ is described using five fuzzy subsets called membership functions: N_{i2}, N_{i1}, Z_i, P_{i1} and P_{i2}, this input variable indicates two main information, the sign of error $(\mu.x_{p_m})$ and its amplitude. Similarly, to output variable $\Delta\hat{v}_w(k)$, we have five fuzzy subsets N_{o2}, N_{o1}, Z_o, P_{o1} and P_{o2}. Triangular symmetrical memberships functions are selected for the input and output variables as shown in Figure (3). The designed *FLC* uses five fuzzy control rules. The used fuzzy rules here have the form of "*If-Then*"; and are designed and represented as below:

- *If* $\mu.x_{p_m}$ *is* N_{i2} *Then* $\Delta\hat{v}_w(k)$ *is* N_{o2}
- *If* $\mu.x_{p_m}$ *is* N_{i1} *Then* $\Delta\hat{v}_w(k)$ *is* N_{o1}
- *If* $\mu.x_{p_m}$ *is* Z_i *Then* $\Delta\hat{v}_w(k)$ *is* Z_o
- *If* $\mu.x_{p_m}$ *is* P_{i1} *Then* $\Delta\hat{v}_w(k)$ *is* P_{o1}
- *If* $\mu.x_{p_m}$ *is* P_{i2} *Then* $\Delta\hat{v}_w(k)$ *is* P_{o2}

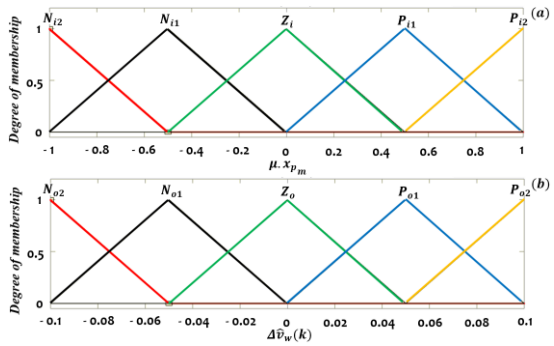

Figure 3. a. Input variable membership functions, b. Change of the estimated wind speed $(\Delta\hat{v}_w(k))$ membership functions

The output of the *FLC* is a fuzzy subset of control. A nonfuzzy values are required for the control, that can be done by using a *defuzzification* method. *Defuzzification* is the process of converting a fuzzified output into a single crisp value. This operation is performed by using the centroid method.

4. IMPROVED MRAS OBSERVER BASED ON SLIDING MODE CONTROLLER ADAPTATION MECHANISM

A Model Reference Adaptive Speed (*MRAS*) observer as shown in Figure (4) is composed of two models, a reference model built from the ψ_{ds} and ψ_{qs} equations, and an adaptive model given by equations (20) and (21).

$$\hat{\psi}_{ds} = \int \left(V_{ds} - R_s \hat{I}_{ds} + \hat{\omega}_r L_q \hat{I}_{qs}\right) dt + \psi_0 \quad (20)$$

$$\hat{\psi}_{qs} = \int \left(V_{qs} - R_s \hat{I}_{qs} - \hat{\omega}_r L_d \hat{I}_{ds} - \psi_0 \hat{\omega}_r\right) dt \quad (21)$$

The used adaptation mechanism in the conventional *MRAS* observer is based on constant gain proportional integral (*PI*) controller; the objective is to drive the output error vector between the reference and the adaptive model to zero. The error in the *d-q* coordinates is defined as: $[\varepsilon_{\omega_{r1}}, \varepsilon_{\omega_{r2}}]^T = [\hat{\psi}_{ds} - \psi_{ds}, \hat{\psi}_{qs} - \psi_{qs}]^T$.

The estimated speed is given as follows:

$$\hat{\omega}_r = k_p\left(\varepsilon_{\omega_{r1}} . \hat{\psi}_{qs} - \varepsilon_{\omega_{r2}} . \hat{\psi}_{ds}\right) + k_i \int \left(\varepsilon_{\omega_{r1}} . \hat{\psi}_{qs} - \varepsilon_{\omega_{r2}} . \hat{\psi}_{ds}\right) dt + \omega_r(0) \quad (22)$$

$$Where: \varepsilon_{\omega_{r1}} . \hat{\psi}_{qs} - \varepsilon_{\omega_{r2}} . \hat{\psi}_{ds} = \psi_{qs} . \hat{\psi}_{ds} - \psi_{ds} . \hat{\psi}_{qs} \quad (23)$$

In order to improve the *MRAS* observer estimation performance, an adaptive mechanism based on sliding mode controller is considered (Gadoue et al., 2009).

The sliding surface is defined as follows:

$$S = \varepsilon_{\omega_r} + \int k \varepsilon_{\omega_r} dt, \quad (k > 0)$$
$$Where: \varepsilon_{\omega_r} = \hat{\psi}_{ds}\psi_{qs} - \hat{\psi}_{qs}\psi_{ds} \quad (24)$$

The sliding surface is equal to zero $(S = 0)$ when the system is in the sliding mode. The first derivative of S gives:

$$\dot{S} = \dot{\varepsilon}_{\omega_r} + k\varepsilon_{\omega_r} \quad (25)$$

When the system reaches the sliding surface, we have $\dot{S} = 0$, therefore the error dynamics can be expressed as:

$$\dot{\varepsilon}_{\omega_r} = -k\varepsilon_{\omega_r} \quad (26)$$

The sliding mode control law is determined using the *Lyapunov* theory, we have:

$$v = \frac{1}{2} s^2 \quad (27)$$

The system is globally stable, if the derivative of the *Lyapunov* function is negative $(\dot{v} < 0)$. The derivative of the *Lyapunov* function gives:

$$\dot{v} = S\dot{S} \iff S(\dot{\varepsilon}_{\omega_r} + k\varepsilon_{\omega_r}) \quad (28)$$

The derivation of error ε_{ω_r} gives:

$$\dot{\varepsilon}_{\omega_r} = \dot{\hat{\psi}}_{ds}\psi_{qs} + \hat{\psi}_{ds}\dot{\psi}_{qs} - \dot{\hat{\psi}}_{qs}\psi_{ds} - \hat{\psi}_{qs}\dot{\psi}_{ds} \quad (29)$$

By replacing Equations (20) and (21) into Equation (29), error derivative $(\dot{\varepsilon}_{\omega_r})$ becomes:

$$\dot{\varepsilon}_{\omega_r} = \hat{\psi}_{ds}\dot{\psi}_{qs} - \hat{\psi}_{qs}\dot{\psi}_{ds} + V_{ds}\psi_{qs} - R_s\hat{I}_{ds}\psi_{qs} + \hat{\omega}_r L_q \hat{I}_{qs}\psi_{qs} - V_{qs}\psi_{ds} + R_s\hat{I}_{qs}\psi_{ds} + \hat{\omega}_r L_d \hat{I}_{ds}\psi_{ds} + \psi_{ds}\hat{\omega}_r\psi_0$$
$$\dot{\varepsilon}_{\omega_r} = \hat{\psi}_{ds}\dot{\psi}_{qs} - \hat{\psi}_{qs}\dot{\psi}_{ds} + \psi_{qs}\left(V_{ds} - R_s\hat{I}_{ds}\right) - \psi_{ds}\left(V_{qs} - R_s\hat{I}_{qs}\right) + \hat{\omega}_r(L_q\hat{I}_{qs}\psi_{qs} + L_d\hat{I}_{ds}\psi_{ds} + \psi_{ds}\psi_0) \quad (30)$$

Let f_1 and f_2 be defined as:

$$f_1 = \hat{\psi}_{ds}\dot{\psi}_{qs} - \hat{\psi}_{qs}\dot{\psi}_{ds} + \psi_{qs}\left(V_{ds} - R_s\hat{I}_{ds}\right) - \psi_{ds}\left(V_{qs} - R_s\hat{I}_{qs}\right) \quad (31)$$

$$f_2 = L_q\hat{I}_{qs}\psi_{qs} + L_d\hat{I}_{ds}\psi_{ds} + \psi_{ds}\psi_0 = \hat{\psi}_{qs}\psi_{qs} + \hat{\psi}_{ds}\psi_{ds} \quad (32)$$

Where: $\hat{\psi}_{qs} = L_q\hat{I}_{qs}$ *And* $\hat{\psi}_{ds} = L_d\hat{I}_{ds} + \psi_0$ (33)

$$\dot{S} = \dot{\varepsilon}_{\omega_r} + k\varepsilon_{\omega_r} = f_1 + f_2\hat{\omega}_r + k\varepsilon_{\omega_r} \quad (34)$$

By substituting Equation (34) into Equation (28), we obtain the final expression of the *Lyapunov* function derivative($\dot{v}$):

$$\dot{v} = S\dot{S} = S(f_1 + f_2\hat{\omega}_r + k\varepsilon_{\omega_r}) \quad (35)$$

The *Lyapunov* function derivative ($\dot{v}$) is negative if:

$$\left(f_1 + f_2\hat{\omega}_r + k\varepsilon_{\omega_r}\right) \begin{matrix} < 0 & for & S > 0 \\ = 0 & for & S = 0 \\ > 0 & for & S < 0 \end{matrix} \quad (36)$$

The general *SMC* form contains an equivalent control $u_{eq}(t)$ used to keep the system state on the sliding surface and a switching control $u_s(t)$ used to forces the system sliding on this surface. The *SMC* law is given as follows:

$$u(t) = u_{eq}(t) + u_s(t) \quad (37)$$

The equivalent and the switching control functions are expressed as follows:

$$u_s(t) = Msign(S), \qquad M > 0 \quad (38)$$

$$u_{eq}(t) = \frac{-f_1 - k\varepsilon_{\omega_r}}{f_2} \quad (39)$$

Where M is the hitting control gain. The rotational speed can be estimated using the following law:

$$\hat{\omega}_r = \frac{-f_1 - k\varepsilon_{\omega_m}}{f_2} + Msign(S) \quad (40)$$

$$Where: sign(S) = \begin{cases} -1 & for \quad S < 0 \\ +1 & for \quad S > 0 \end{cases} \quad (41)$$

The sign function in equation (40) has been replaced by the sigmoid function $H(s)$, in order to reduce the chattering phenomenon. Function f_2 may cause an estimation errors when its value approaches zero, because of its presence in the denominator of equivalent control $u_{eq}(t)$, this problem is solved by adding a small positive constant to f_2. The final estimated rotational speed expression is given as follows:

$$\begin{cases} \hat{\omega}_r = \dfrac{-f_1 - k\varepsilon_{\omega_m}}{f_2} + M.H(s) \\ H(s) = \left[\dfrac{2}{(1 + e^{-sx})}\right] - 1 \end{cases} \quad (42)$$

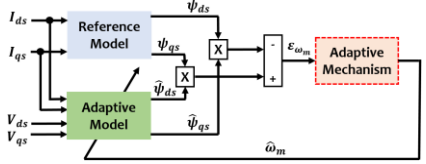

Figure 4. Model reference adaptive speed (*MRAS*) Observer

5. CONTROLLER DESIGN

Two control loops were designed (Figure 8), an outer control loop based on fuzzy super twisting algorithm used to regulate the generator speed to its optimal value and to provide the optimum *DC* side current, and an internal control loop based on sliding mode controller used to regulate the *DC* side current to its optimal value and to provide the appropriate signal for the *DC-DC* boost converter.

✓ *Generalized Super-Twisting Algorithm*

According to (Moreno et al., 2008), the generalized *STA* can be described by the following differential inclusion:

$$\begin{cases} \dot{\sigma} = -k_1\phi_1(\sigma) + z & (\sigma \in \mathbb{R}) \\ \dot{z} = -k_2\phi_2(\sigma) + \varrho(t) & (z \in \mathbb{R}) \end{cases} \quad (43)$$

The nonlinear stabilizing terms are given as follows:

$$\begin{cases} \phi_1(\sigma) = \mu_1|\sigma|^{\frac{1}{2}}sgn(\sigma) + \mu_2\sigma, \\ \quad with \quad \mu_1, \mu_2 \geq 0 \\ \phi_2(\sigma) = \dfrac{{\mu_1}^2}{2}sgn(\sigma) + \dfrac{3}{2}\mu_1\mu_2|\sigma|^{\frac{1}{2}}sgn(\sigma) \\ \quad + {\mu_2}^2\sigma \end{cases} \quad (44)$$

μ_1 can take only the value $\mu_1 = 1$ and $\mu_1 = 0$.

✓ *Fuzzy-VGSTA Speed Controller design for PMSG:*

The speed tracking error (sliding surface) and its reachability condition are defined as follows:

$$\begin{cases} S_{\Omega_m^G} = \varepsilon_x = \hat{\Omega}_{mopt}^G - \hat{\Omega}_m^G \\ S_{\Omega_m^G}\dot{S}_{\Omega_m^G} < 0 \end{cases} \quad (45)$$

Where $\hat{\Omega}_{mopt}^G$ is the reference rotational speed ($\hat{\Omega}_{mopt}^G = {(\hat{v}_w.\lambda^*)}/{R}$) and λ^* is the optimum tip-speed ratio.

The first order and the second order sliding mode control for Ω_m^G are given respectively by:

$$\begin{aligned} \dot{S}_{\Omega_m^G} &= \dot{\hat{\Omega}}_{mopt}^G - \left[\frac{1}{J^G}\left(T_m^G - f.\hat{\Omega}_m^G - T_{em}^G\right)\right] \\ &= \dot{\hat{\Omega}}_{mopt}^G - \left[\frac{1}{J^G}\left(T_m^G - f.\hat{\Omega}_m^G - k_bI_m\right)\right] \\ \ddot{S}_{\Omega_m^G} &= \ddot{\hat{\Omega}}_{mopt}^G + \frac{k_b}{J^G}\dot{I}_m + \frac{f}{J^G}\dot{\hat{\Omega}}_m^G - \frac{\dot{T}_m^G}{J^G} \end{aligned} \quad (46)$$

According to (Yin, Xiu-xing, et al., 2015) the electromagnetic torque can be approximated by: $T_{em}^G = k_bI_m$.

Considering a single input and a single output nonlinear system (Das et al., 2018) $\dot{S}_{\Omega_m^G} = f\left(t, S_{\Omega_m^G}\right) + u$, where $f\left(t, S_{\Omega_m^G}\right)$ is unknown bounded perturbation term and globally bounded by $\left|f\left(t, S_{\Omega_m^G}\right)\right| \leq \partial\left|S_{\Omega_m^G}\right|^p$ for some constant $\partial > 0$. The maximum sliding order as *2* can be reached by choosing p as *0.5*.

Control input I_{m_opt} for Ω_m^G by applying the variable gain super twisting algorithm is given as follows:

$$\sigma = z_1\dot{S}_{\Omega_m^G} + z_2\left|S_{\Omega_m^G}\right|^{\frac{1}{2}}sgn\left(S_{\Omega_m^G}\right), \ with\, z_1, z_2 > 0$$

$$\tilde{\mathcal{L}} = -k_1(\sigma, t)\phi_1(\sigma) - \int_0^t k_2(\sigma, t)\phi_2(\sigma)dt$$

$$\begin{cases} \phi_1(\sigma) = |\sigma|^{\frac{1}{2}}sgn(\sigma) + \mu_2\sigma, with \quad \mu_2 > 0 \\ \phi_2(\sigma) = \dfrac{1}{2}sgn(\sigma) + \dfrac{3}{2}\mu_2|\sigma|^{\frac{1}{2}}sgn(\sigma) + {\mu_2}^2\sigma \\ k_1 = \partial\left|z_1\dot{\varepsilon}_x + z_2|\varepsilon_x|^{\frac{1}{2}}sgn(\varepsilon_x)\right|^n = \partial|\sigma|^n \\ k_2 = \eta\left|z_1\dot{\varepsilon}_x + z_2|\varepsilon_x|^{\frac{1}{2}}sgn(\varepsilon_x)\right|^m = \eta|\sigma|^m \end{cases} \quad (47)$$

When *STA* gains k_1 and k_2 are constant and $\mu_2 = 0$ the standard *STA* is recovered. $\mu_2 > 0$ allows to handle with disturbances and perturbations that grow outside the sliding surface and the variable gains k_1 and k_2 make possible to render the sliding surface insensitive to bounded perturbations. ∂ and η are super twisting algorithm tuning parameters. To allow a good dealing with the random wind speed nature, ∂ has been considered here as an additional adaptive parameter. The ∂ value should vary according to the wind speed (v_w) variation. A *sugeno FLC* is selected for this purpose. The input of the considered *FLC* has two inputs. The first one is the estimated wind speed value provided by the fuzzy wind speed estimator ($\hat{v}_w(k)$) and the second one is the change of the estimated wind speed ($\Delta\hat{v}_w(k) = \hat{v}_w(k) - \hat{v}_w(k-1)$). The *FLC* provides as output the *VGSTA* tuning parameter ($\partial(k)$). *FLC* input variables have been divided and assigned to the linguistic variables using nine fuzzy membership functions: $r_1, r_2, r_3, r_4, r_5, r_6, r_7, r_8$ and r_9 for the estimated wind speed variable, and three linguistic variables N, Z and P for the estimated wind speed change. The output variable $\partial(k)$ has been also divided and assigned to the linguistic variables using seven fuzzy subsets O_{i1}, O_{i2}, O_{i3}, O_{i4}, O_{i5}, O_{i6}, O_{i7}, O_{i8} and O_{i9}. The common triangular

symmetrical memberships functions have been used for the *FLC* variables (Figures (5),(6) and (7)). The fuzzy rules have the form of "*If-Then*" with "*and*" logical operator, and are represented as below:

- *If* $\hat{v}_w(k)$ *is* r_1 *and* $\Delta\hat{v}_w(k)$ *is (N Or Z) Then* $\partial(k)$ *is* O_{i1}
- *If* $\hat{v}_w(k)$ *is* r_1 *and* $\Delta\hat{v}_w(k)$ *is P Then* $\partial(k)$ *is* O_{i2}
- *If* $\hat{v}_w(k)$ *is* r_2 *and* $\Delta\hat{v}_w(k)$ *is (N Or Z) Then* $\partial(k)$ *is* O_{i2}
- *If* $\hat{v}_w(k)$ *is* r_2 *and* $\Delta\hat{v}_w(k)$ *is P Then* $\partial(k)$ *is* O_{i3}
- *If* $\hat{v}_w(k)$ *is* r_3 *and* $\Delta\hat{v}_w(k)$ *is (N Or Z) Then* $\partial(k)$ *is* O_{i3}
- *If* $\hat{v}_w(k)$ *is* r_3 *and* $\Delta\hat{v}_w(k)$ *is P Then* $\partial(k)$ *is* O_{i4}
- *If* $\hat{v}_w(k)$ *is* r_4 *and* $\Delta\hat{v}_w(k)$ *is (N Or Z) Then* $\partial(k)$ *is* O_{i4}
- *If* $\hat{v}_w(k)$ *is* r_4 *and* $\Delta\hat{v}_w(k)$ *is P Then* $\partial(k)$ *is* O_{i5}
- *If* $\hat{v}_w(k)$ *is* r_5 *and* $\Delta\hat{v}_w(k)$ *is (N Or Z) Then* $\partial(k)$ *is* O_{i5}
- *If* $\hat{v}_w(k)$ *is* r_5 *and* $\Delta\hat{v}_w(k)$ *is P Then* $\partial(k)$ *is* O_{i6}
- *If* $\hat{v}_w(k)$ *is* r_6 *and* $\Delta\hat{v}_w(k)$ *is (N Or Z) Then* $\partial(k)$ *is* O_{i6}
- *If* $\hat{v}_w(k)$ *is* r_6 *and* $\Delta\hat{v}_w(k)$ *is P Then* $\partial(k)$ *is* O_{i7}
- *If* $\hat{v}_w(k)$ *is* r_7 *and* $\Delta\hat{v}_w(k)$ *is (N Or Z) Then* $\partial(k)$ *is* O_{i7}
- *If* $\hat{v}_w(k)$ *is* r_7 *and* $\Delta\hat{v}_w(k)$ *is P Then* $\partial(k)$ *is* O_{i8}
- *If* $\hat{v}_w(k)$ *is* r_8 *and* $\Delta\hat{v}_w(k)$ *is (N Or Z) Then* $\partial(k)$ *is* O_{i8}
- *If* $\hat{v}_w(k)$ *is* r_8 *and* $\Delta\hat{v}_w(k)$ *is P Then* $\partial(k)$ *is* O_{i9}
- *If* $\hat{v}_w(k)$ *is* r_9 *and* $\Delta\hat{v}_w(k)$ *is (N Or Z Or P) Then* $\partial(k)$ *is* O_{i9}

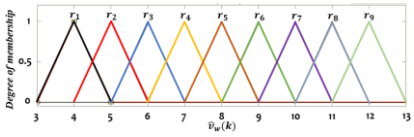

Figure 5. Estimated wind speed ($\hat{v}_w(k)$) membership functions

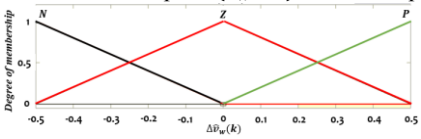

Figure 6. Change of the estimated wind speed ($\Delta\hat{v}_w(k)$) membership functions

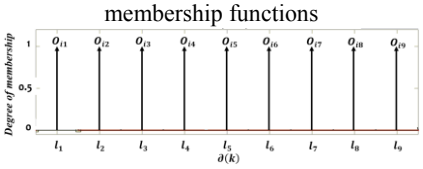

Figure 7. Tuning parameter (∂) membership functions

For this *Sugeno-style* inference the *defuzzification* is performed using the *weighted average* method.

✓ *Current Loop Controller:*

To control the *PMSG* based *WECS*, an appropriate signal for *DC-DC* boost converter is required. The current controller used here for this purpose is based on sliding mode controller (*SMC*). The *DC-DC* boost depicted in Figure (1) can be represented by the following dynamic equations:

$$\begin{cases} \dot{I}_m = -\dfrac{r_m}{L_m} I_m + \dfrac{1}{L_m} V_{dc} - \dfrac{(1-q)}{L_m} V_{aM} \\ \dot{V}_{dc} = \dfrac{1}{C_e} I_{dc} - \dfrac{1}{C_e} I_m \end{cases} \quad (48)$$

Where I_m is the input current, V_{aM} is the output voltage, V_{dc} is the input voltage, q is the switch state, L_m and C_e are energy storage elements and r_m is the internal resistance of the boost inductance L_m.

The *DC-DC* boost converter is forced to bring up the *PMSG* to operate at the optimum *DC*-side current I_{m_opt} and therefore at the maximum power working point (*MPP*). The sliding surface σ_{I_m} and the control law are defined as follows:

$$\sigma_{I_m} = I_{m\_opt} - I_m$$

$$q = \frac{1}{2}\left[1 + Sign(\sigma_{I_m})\right], with\ q = \begin{cases} 1 & \sigma_{I_m} > 0 \\ 0 & \sigma_{I_m} < 0 \end{cases} \quad (49)$$

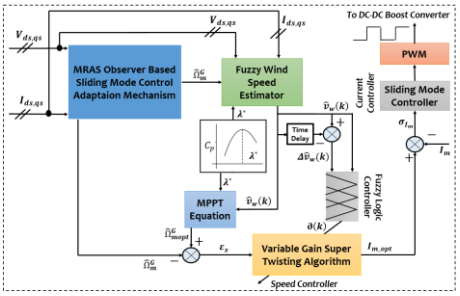

Figure 8. Proposed sensorless control strategy

6. RESULTS & DISCUSSION

The test has been performed by replacing the physical sensors by the improved *MRAS* speed observer and the fuzzy wind speed estimator. The overall fully sensorless control strategy have been investigated under random wind speed profile. The wind speed was modeled as a sum of deterministic several harmonics. Figure (9) represents the applied random wind speed profile and the estimated one by the fuzzy wind speed estimator using the second input information, the fuzzy wind speed estimator shows a high estimation performance with a very small error. Figure (10) depicts the response of the *MRAS* speed observer, we can notice, a high estimation accuracy of the generator speed at dynamic and steady state regime. Figure (11) depicts the variation of the power coefficient (C_p) of the proposed fully sensorless *MPPT* strategy. As can be seen the power coefficient is kept close to its optimum value 0.48 even under arbitrary wind speed profile. The proposed control strategy has been compared to the conventional simple sensorless *MPPT* strategy presented in many research papers (Hussein, Mahmoud M., et al., 2010). The concept of this latter is based on perturbing the control variable (duty-cycle of the *DC-DC* boost converter) using a fixed step-size and observing the resulting power changes until achieving the maximum power point. Even that this technique is simple, flexible and does not require any knowledge about the wind turbine characteristic; its main drawback is the poor stability around the *MPP* and it fails to achieve the maximum power under sudden wind variations. These drawbacks has been observed on the studied system when applying this technique, the obtained power coefficient (C_p) using the conventional method is shown in Figure (11), we notice large oscillations around the maximum power coefficient, the thing which lead to affect the captured mechanical power (Figure (12)) and causes a vibration and noise of the machines. Figures (13) and (14) shows the motor-pump performances using the proposed and conventional *MPPT* strategy, the first one depict the variation of the absorbed power by the motor-pump group and the second one represents the variation of the electrical torque and the load torque opposed by the centrifugal pump. From the obtained results, it can be noted that under random wind speed profile, the conventional control strategy gives higher ripple in power and torques of the motor pump group caused due to oscillation around the maximum power point, it can be also noted that this oscillations are almost negligible using the proposed *MPPT* control strategy and applying this latter will ensure a stable working of the pumping system without any vibrations or noises of the motors.

CONCLUSIONS

A fully robust sensorless control strategy has been proposed in this paper for a direct-drive *PMSG* wind turbine. The studied

system is supposed supplying a water pumping system. Unlike the resistive load, the motor-pump unit has a nonlinear behavior; the applied conventional *MPPT* controller in this case has shown large ripples at the captured mechanical power and at the absorbed power level. The obtained results showed that the proposed sensorless control ensures high tracking performance, high stability under random wind speed profile and could greatly reduce the ripples that appear when applying the classical *MPPT* strategy.

REFERENCES

Fernandez, R. D., R. J. Mantz, and P. E. Battatotto. "Sliding mode control for efficiency optimization of wind electrical pumping systems." Wind Energy: An International Journal for Progress and Applications in Wind Power Conversion Technology 6.2 (2003): 161-178.

Qiao, Wei, Xu Yang, and Xiang Gong. "Wind speed and rotor position sensorless control for direct-drive PMG wind turbines." IEEE Transactions on Industry Applications 48.1 (2011): 3-11.

Sitharthan, R., et al. "Adaptive hybrid intelligent MPPT controller to approximate effectual wind speed and optimal rotor speed of variable speed wind turbine." ISA transactions (2019).

Belmokhtar, Karim, Mamadou Lamine Doumbia, and Kodjo Agbossou. "Novel fuzzy logic based sensorless maximum power point tracking strategy for wind turbine systems driven DFIG (doubly-fed induction generator)." Energy 76 (2014): 679-693.

Mohamed, Mansouri, et al. "New hybrid sensorless speed of a non-salient pole PMSG coupled to wind turbine using a modified switching algorithm." ISA transactions (2019).

Kot, Radoslaw, Michal Rolak, and Mariusz Malinowski. "Comparison of maximum peak power tracking algorithms for a small wind turbine." Mathematics and Computers in Simulation 91 (2013): 29-40.

Gadoue, Shady M., Damian Giaouris, and John W. Finch. "MRAS sensorless vector control of an induction motor using new sliding-mode and fuzzy-logic adaptation mechanisms." IEEE Transactions on Energy Conversion 25.2 (2009): 394-402.

Moreno, Jaime A., and Marisol Osorio. "A Lyapunov approach to second-order sliding mode controllers and observers." 2008 47th IEEE conference on decision and control. IEEE, 2008.

Yin, Xiu-xing, et al. "A novel fuzzy integral sliding mode current control strategy for maximizing wind power extraction and eliminating voltage harmonics." Energy 85 (2015): 677-686.

Das, S., & Subudhi, B. (2018). A ${H_\infty} $ Robust Active and Reactive Power Control Scheme for a PMSG-Based Wind Energy Conversion System. IEEE Transactions on Energy Conversion, 33(3), 980-990.

Hussein, Mahmoud M., et al. "Simple sensorless control technique of permanent magnet synchronous generator wind turbine." 2010 IEEE International Conference on Power and Energy. IEEE, 2010.

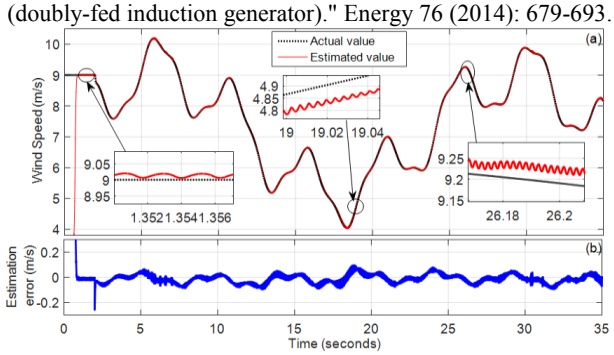

Figure 9. Actual and estimated wind speed profile

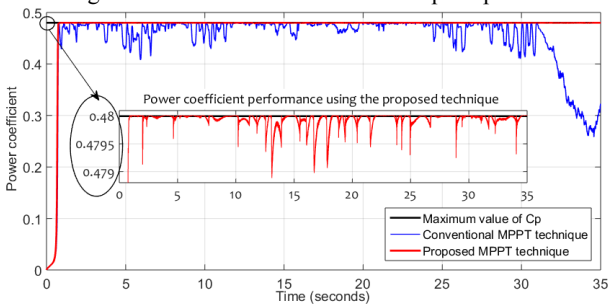

Figure 11. Power coefficient and its optimal reference

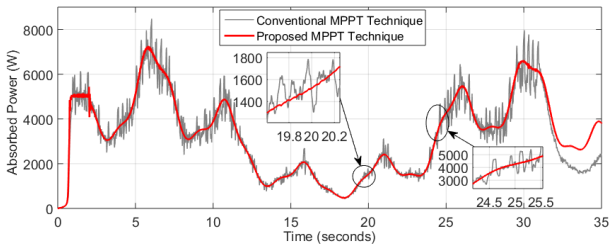

Figure 13. Absorbed power by motor-pump group

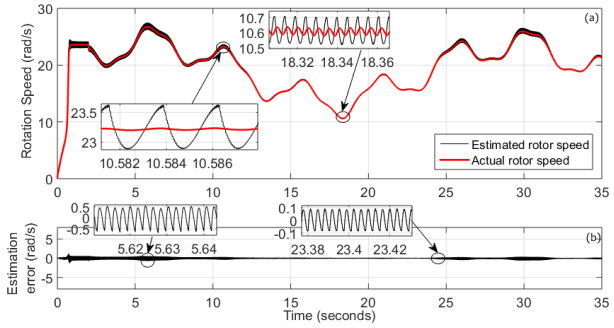

Figure 10. Actual and estimated rotational speed

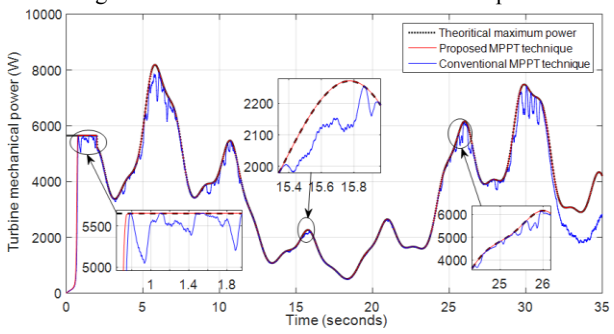

Figure 12. Variation of the turbine mechanical power

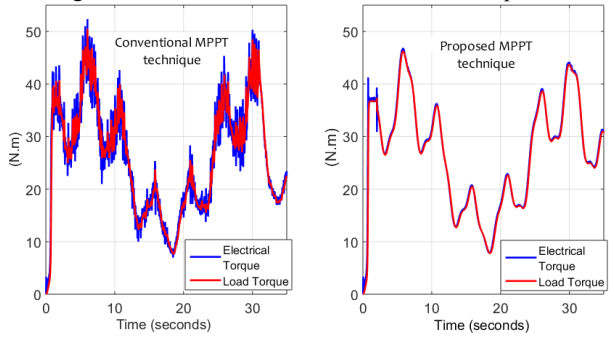

Figure 14. Electrical and load torque of the motor-pump